ARTICLE

Study on Coconut Shell Activated Carbon Temperature Swing Adsorption of Benzene and Formaldehyde

Zhiguang Yang[1,*], Gaojun Yan[1,2], Xueping Liu[1], Zhengyuan Feng[1], Xinfeng Zhu[1], Yanli Mao[1], Songtao Chen[1], Zhisheng Yu[2], Ruimei Fan[3] and Linlin Shan[3,*]

[1]Henan Province Key Laboratory of Water Pollution Control and Rehabilitation Technology, Henan University of Urban Construction, Pingdingshan, 467036, China

[2]College of Resources and Environment, University of Chinese Academy of Sciences, Beijing, 100085, China

[3]College of Basic Medical Sciences, Xinxiang Medical University, Xinxiang, 453003, China

[*]Corresponding Authors: Zhiguang Yang. Email: yangzhiguang@hncj.edu.cn; Linlin Shan. Email: shanlinlin@xxmu.edu.cn

ABSTRACT

Adsorption can be used to recover effectively the volatile organic gases (VOCs) in the exhaust gas from factories through using an appropriate adsorption bed. Due to form a physical or chemical bond, adsorption occurs between the porous solid medium and the liquid or gas multi-component fluid mixture. The regeneration capacity of the adsorbent is as important as the adsorption capacity and it determines the economics of the adsorption system. The regeneration of adsorbent can be realized through changing the pressure or temperature of the system. Here, activated carbon samples from coconut shell were prepared and characterized. Benzene or formaldehyde in the mixed air was used as the adsorption object, and the adsorption experiment was carried out in a U-shaped bed. Discussed how adsorption was affected by activated carbon type, adsorbate and temperature. The results show that oxidation modified activated carbon can increase the adsorption effect of formaldehyde, but will reduce the adsorption effect of benzene, because their adsorption mechanism is different. At 30°C, the saturated adsorption capacity of AC-0 for benzene is 437.0 mg/g, and that of AC-1 for formaldehyde is 670.5 mg/g. In the experimental range, it is found that the adsorption capacity increases with the decrease of temperature, and their changes are very consistent with the fitted ExpDecay1 function.

KEYWORDS

Activated carbon; adsorption; benzene; formaldehyde; oxidation modification

Nomenclature

AC-0   Activated carbon from coconut shell
AC-1   Activated carbon after oxidation

1 Introduction

With the continual development of society, volatile organic compounds (VOCs) have gradually become the most widely distributed and diverse of exhaust emissions, with the exception of particulate matter [1]. So,

VOCs have become one of the most important air pollutants [2]. These pollutants have caused serious harm to the human body, human production and general living space. Benzene series and formaldehyde are the air pollutants strictly controlled by the national standard.

At the present, the treatment of VOCs can be divided into two categories [3]. One is the destructive method [4–6], the main purpose of which is to convert VOCs into CO_2 and H_2O. The other is the non-destructive method, such as adsorption [7], whose main purpose is separation and recycling. The adsorption method has the characteristics of energy-saving, high efficiency, and economy. It is one of the effective control methods for low concentration VOCs, and is a hotspot of research and application at present [8].

Adsorption can be divided into physical adsorption and chemical adsorption, according to the different forces between the surface of the adsorbent and the adsorbed substance. Physical adsorption refers to the force between the adsorbed substance molecules in the fluid and the active groups on the surface of the solid adsorbent, which is caused by the intermolecular attraction, namely "van der Waals force"; several ad-sorbent layers with a molecular thickness (multi molecule) or single-molecule thickness can be formed on the surface of the adsorbent; the adsorption speed is very fast, and the balance between phases can be achieved in an instant; the adsorption process is similar to the physical process of gas condensation, and the heat released is equivalent to the condensation heat of gas. If the gas pressure decreases or the system temperature increases, the adsorbed gas can easily escape from the solid surface without changing the original characteristics of the gas. This phenomenon is called desorption. Adsorption and desorption can be reversible processes under some conditions. This reversibility can be used within industry, by changing the operating conditions to desorb the adsorbed material, thereby regenerating, recovering or removing the adsorbed material [9].

Activated carbon is a powerful adsorbent. Its uniqueness and versatility make it widely used [10–13]. Quite diverse source materials are currently used in active carbon production, such as oil palm empty fruit bunches [14], walnut shells [15], starches [16], rice husks [17], coconut husks [18], etc.

Activated carbon will exhibit extremely strong application properties through structural changes. The main methods of modifying the surface physical structures of activated carbon include the chemical method, physical method, and physicochemical method [19–23]. Oxidation modification is to oxidize the chemical structure (functional group structure) on the surface of activated carbon by using strong oxidants, which significantly change the chemical structure of the surface of activated carbon.

Among the factors that affect the adsorption, appropriately increasing the pressure or lowering the temperature is beneficial to improve the adsorption effect while lowering the pressure or raising the temperature is beneficial to desorption. Other properties of the adsorbent (such as specific surface area) also have a greater impact on the adsorption effect, and a larger specific surface area is an effective means of further increasing adsorption. On the other hand, the nature of the adsorbate (such as the polarity of the adsorbate) also affects the entire adsorption process. Just like our previous work [24], most newer studies are now paying considerable attention to the investigation of the isothermal adsorption equilibrium and its kinetics [25–28]. However, in many industrial applications, temperature swing adsorption systems are widely used [29]. Adam et al. [30] introduced the effects of aging in industrial-scale temperature-swing adsorption for gas cleaning in biomass gasification. Han et al. [31] studied the adsorption and desorption behaviors of two polar-nonpolar typical VOCs (n-butyl acetate and xylene) on activated carbon by a temperature swing-vacuum pressure swing adsorption hybrid process.

In the previous existing work, although research and progress have been made in the adsorption of biochar derived from biomass to VOCs, there are still some limitations and deficiencies. Some such as small specific surface area; Poor regeneration performance; The adsorption of different polar adsorbents is unstable.

In this study, coconut shell activated carbon, a kind of VOCs adsorbent with good regeneration performance, was prepared by using coconut shell as raw material. The temperature swing adsorption

processes of benzene and formaldehyde on activated carbon were studied, and the relationship between the structure of activated carbon and adsorption was explored. Activated carbon shows a good prospect for industrial application and achieves the goal of "treating waste with waste".

2 Materials and Methods

2.1 Materials and Instruments

The coconut shell used in the experiment was purchased from the fruit market. Nitric acid, concentrated sulfuric acid, sodium hydroxide, and the potassium permanganate used in the experiment were analytically pure and purchased from Shanghai Sinopharm Chemical Reagent Co., Ltd., China. The adsorbates used in this experiment were benzene and formaldehyde, and their physical and chemical properties are shown in Table 1.

Table 1: Physical and chemical properties of benzene and formaldehyde

Adsorbate	Molecular weight (g/mol)	Relative density (g/cm^3)	Melting point (°C)	Boiling point (°C)	Saturated vapor pressure (KPa, 30°C)	Polarity
Benzene	78.11	0.88	5.5	80.1	13.33	Nonpolar
Formaldehyde	30.3	0.815	−92	−19.5	13.33	Polar

The detector is manufactured by RAE Systems Inc. with the model being a pgm-7300; the specific surface area and pore diameter tester is manufactured by Micromeritics instrument Ltd., China. with the model being the ASAP 2020; the tubular furnace is manufactured by Nobody Materials Ltd., China. with the model being nbd-o1200; the Fourier transform infrared spectrometer is manufactured by Thermo Fisher Scientific-CN, the model being the Nicolet Is10.

2.2 Experimental Device

The device (Fig. 1) used in the adsorption experiment is a self-made U-shaped adsorption column, its inner diameter is 1.0 cm, the length of activated carbon bed is about 9 cm, the mass of activated carbon is 1.0000 g, and the temperature is controlled by a water bath.
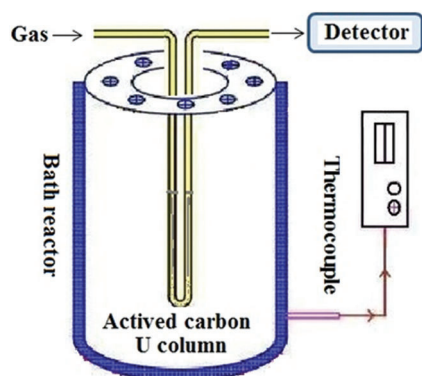

Figure 1: The device used in the adsorption experiment

2.3 Experimental Methods

Put the cleaned coconut shell in the oven and dry it at 105°C for 1 h. After that, crush and sift it with 80 mesh sieves. Undersized power (particle size less than 0.18 mm) was collected and used as the next pyrolysis material. Coconut shell powder was placed in a quartz boat, and then in a muffle furnace, the

temperature was programmed (20 °C/min) to 400°C under the protection of nitrogen for 2 h. After carbonization, the product was cooled to room temperature, and then put into a pressure sterilization pot with 1 M NaOH solution at a solid-liquid ratio of 1/10, a temperature of 120°C for 1 h, then taken out, and repeatedly washed with distilled water till the pH of the filtrate was nearly neutral. Then, the alkali treatment product was put into a pressure sterilization pot with 1 M HNO_3 solution at a solid-liquid ratio of 1/10, and treated at 120°C for 1 h, then filtrated, and repeatedly washed with distilled water till the pH of the filtrate was neutral. Put it into the electric blast oven, and dry it at 105°C for 1 h, screen 100–120 mesh, and this product should be labeled as AC-0 [30].

The potassium permanganate solution with 0.05% mass concentration was prepared. The AC-0 and potassium permanganate solutions were mixed according to the solid-liquid ratio of 1/10 and placed in a pressure sterilization pot, treated at 120°C for 1 h, and then washed and filtered with distilled water 7 times to wash off potassium permanganate. The activated carbon treated with potassium permanganate was placed in an electric blast oven, dried at 105°C for 4 h, then taken out and cooled to room temperature, and the oxidation product is labeled as AC-1. The prepared activated carbon is put into a sealed bag and placed in a dryer for the time being.

Particle sizes of biochar samples (AC-0 and AC-1) range from 0.125 to 0.15 mm. The formations of biochar and activated carbon can be described below (Fig. 2),

Figure 2: The formations of biochar and activated carbon samples

The flow rate of gas containing benzene or formaldehyde was 360 ml/min, and the contents of import and export benzene were detected by VOCs detector (PGM-7300, MiniRAE Lite, RAE Systems, USA). Formaldehyde content is detected by a formaldehyde detector (FP-30, RIKEN, RIKEN Instrument Co., Ltd., Japan). The concentration of imported benzene was 12.8 mg/L, and the concentration of formaldehyde was 8.49 mg/L. The adsorption capacity was obtained by weighing. Each adsorption experiment was carried out three times in parallel, and the average value was taken. The temperature was measured, indicated, and auto-controlled through its matching temperature controller.

The concentration of benzene from the inlet was 12.8 mg/L and the concentration of formaldehyde was 8.49 mg/L in the air atmosphere. So mixed gases are by air (about 99.6%) and benzene (about 0.4%) composition, or by air (about 99.4%) and formaldehyde (about 0.6%) composition.

To investigate whether the adsorptions are influenced by temperature under a normal atmosphere, two groups of experiments were designed and conducted for benzene on AC-0 and formaldehyde on AC-1. The matching process is as follows.

For benzene on AC-0, the concentration of benzene at the inlet was 12.8 mg/L, the flow rate was 360 ml/min, and the adsorption temperature was 10°C for 5 h. Make it reach the adsorption equilibrium (the saturated adsorption capacity is recorded as Q_0), then the adsorption bed is heated at the speed of 10 °C/15min until 100°C, and after that gradually cooled from 100°C to 10°C at the same speed, and weighed every 10°C (adsorption capacity is recorded as Q).

For formaldehyde on AC-1, the concentration of formaldehyde 8.49 mg/L at the inlet was kept, and the airflow velocity was 360 ml/min. Firstly, the adsorption equilibrium was achieved by adsorption at 30°C for 5 h (for the moment, the saturated adsorption capacity was recorded as Q_0), then the adsorption bed was heated intermittently at the rate of 10 °C/15min until 100°C, and then it was cooled intermittently from 100°C to 30°C, and weighed every 10°C (the adsorption capacity was recorded as Q).

2.4 Characterization Methods of the Samples

BET specific surface area, pore volume, and pore size of the samples were analyzed by specific surface area and pore size tester (ASAP2020, Mike Instrument, Micromeritics, USA). The adsorption temperature was 77 K and the adsorption gas was 99.999% high purity nitrogen. Attenuation reflectance Fourier transformation infrared spectrometry (FTIR-8400s, ATR-FTIR, Shimadzu, Japan) was used in analyzes of the sample's functional groups in the range of 4000–400 cm^{-1}. The samples were analyzed by the elemental analyzer to determine the major elements such as carbon (C), hydrogen (H), and oxygen (O). The results of the elemental analysis are summarized in Table 2.

Table 2: The elemental analyses of AC-0 and AC-1 (wt.%)

Samples	Carbon	Hydrogen	Oxygen[a]	Nitrogen
AC-0	92.11	2.68	4.75	0.46
AC-1	90.38	2.52	6.65	0.45

Note: [a]By difference.

3 Results and Discussion

3.1 Characterization of Samples

Fig. 3 shows the adsorption isotherms of AC-0 and AC-1 analyzed by a specific surface area and pore size tester. It can be seen from the figure that the adsorption type of the two samples belongs to type IV in the classification of IUPAC (International Union of Pure and Applied Chemistry). This type describes specific mesoporous materials' adsorption behavior showing the pore condensation of the hysteresis which occurs between the desorption and adsorption branches. In the region of low pressure ($P/P_0 < 0.2$), the curve is convex, and the adsorption and desorption curves coincide, indicating that there exist active sites on the surface of activated carbon and the strong monolayer adsorption of non-polar nitrogen. In the adsorption region of $0.2 < P/P_0 < 0.5$, the adsorption capacity increases slowly with the increase of pressure, and the adsorption and desorption curves still coincide, indicating that the multi-layer adsorption occurs in this region, which can easily occur when the pore size is greater than 20 nm. In the region of $P/P_0 > 0.5$, it can be observed that the adsorption capacity increases rapidly with the increase of pressure, and the adsorption and desorption isotherms of N_2 to samples do not coincide and there is desorption hysteresis, which indicates that the phenomenon of capillary condensation occurs in addition to the multi-layer adsorption.
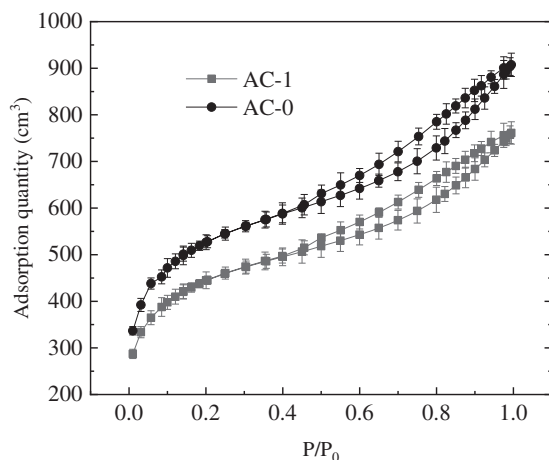
Figure 3: The adsorption balance isotherms of AC-0 and AC-1 on N_2 at 77K

The test results show that the specific surface area of AC-0 is 1860 m^2/g and the pore size of BET is 48.2 nm; the specific surface area of AC-1 is 1564 m^2/g and the pore size of BET is 47.9 nm. The specific surface area and the pore size of AC-1 got a little bit smaller by the oxidation of potassium permanganate. This means that there are much smaller active parts and pore sizes in the pore regarding the appplication of nitrogen onto the active carbon due to plenty of oxygen-containing groups in the pore.

Fig. 4 shows the infrared spectra of the samples before and after oxidation. The broad absorption peak for the alcohol group (O-H bond) was found at around 3370 cm^{-1} and stretching vibration for alcoholic C-O bond was found at 1020 cm^{-1}. 2930 cm^{-1} is the vibration peak of C-H, and vibration peaks of C=C stretching on the aromatic ring were found at 1615 and 1513 cm^{-1}, confirming the presence of the alkene group. The peaks at 1290 cm^{-1} mean epoxy group C-O-C. The strong peak at 878 cm^{-1} is the bend vibration peak of C-H on the aromatic ring. The spectrum also showed the absorption peaks of stretching vibration for the carboxylic acid group at 1700 cm^{-1} for C=O bond. FTIR analysis suggests that the samples have functional groups like alcohol, epoxy, aromatic ring and etc. The infrared spectra of AC-0 and AC-1 are similar, but the oxygen-containing peak of AC-1 is strengthened, indicating that the activated carbon has more oxygen-containing groups after oxidation by potassium permanganate; in other words, it has higher surface polarity.
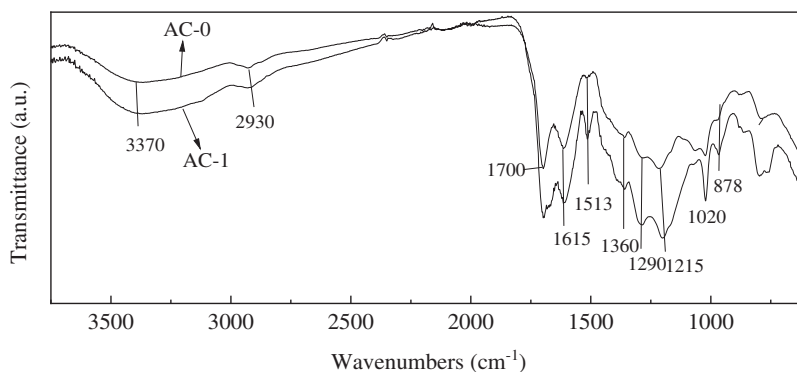

Figure 4: Infrared spectra of activated carbon samples

Samples were analyzed by the elemental analyzer to determine the major elements such as carbon (C), hydrogen (H) and oxygen (O). The results of the elemental analysis are summarized in Table 2. It provides evidence to support AC-1 from the oxidation of AC-0. The O/C atomic ratios measured in the samples ranged from 0.0516 to 0.0736.

3.2 Adsorption of Samples

3.2.1 Saturated Adsorption Capacity of Samples

Under the conditions of 30°C and a normal atmosphere, the experiments show that the saturated adsorption capacity of AC-0 was 437.0 mg/g for benzene and 594.1 mg/g for formaldehyde, and the saturated adsorption capacity of AC-1 for benzene and formaldehyde is 401.6 and 670.5 mg/g, respectively (Table 3). These results mean that the oxidation of activated carbon is not good for the adsorption of benzene, but good for the adsorption of formaldehyde. The primary reason is that they have different adsorption mechanisms. A schematic representation of the adsorption mechanisms of benzene and formaldehyde are shown in Fig. 5. It is physical adsorption for nonpolar benzene by van der Waals force (mainly dispersion force) whereas it is the main chemical adsorption for polar formaldehyde through hydrogen bonds. The van der Waals radius (d_1) of adsorbate will be bigger than the molecular radius (d_2) in the form of a hydrogen bond. Thus the increase of oxygen-containing groups after oxidation is conducive to the increase of formaldehyde adsorption capacity, but adverse to the adsorption of benzene, although the sample AC-1 has a lower specific surface area and pore size. So, the following experiments used AC-0 to adsorb benzene and AC-1 to adsorb formaldehyde.

Table 3: The saturated adsorption capacity of samples at 30°C and normal atmosphere

Sample	Benzene (mg/g)	Formaldehyde (mg/g)
AC-0	437.0[a]	594.1
AC-1	401.6	670.5

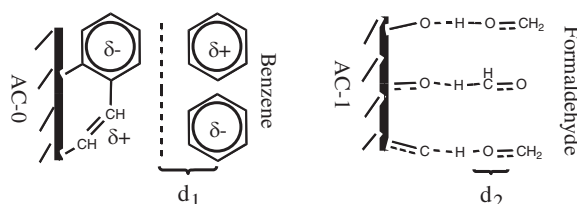Note: [a]This data was reported in Applied Chemical Industry [32].

Figure 5: Schematic representation of adsorption mechanism of benzene and formaldehyde

3.2.2 Adsorption Breakthrough Curves

The prepared activated carbon samples (AC-0 or AC-1) were loaded in a self-made U-shaped adsorption column, and the adsorption experiment for containing simulated polluted gas (benzene or formaldehyde in air) was carried out under the condition of a water bath at 30°C. The adsorption breakthrough curves were obtained by weighing them every 10 min. Fig. 6 is their adsorption breakthrough curves. Both adsorption breakthrough curves fitted by the Logistic model in Origin software are also shown in Fig. 6 [33], and the regression formula is as follows.

$$\frac{C}{C_0} = \frac{A_1 - A_2}{1 + (t/t_0)^P} + A_2 \tag{1}$$

where C is the outlet concentration when the adsorption time is t. C_0 is the gas inlet concentration. Here t is the adsorption time. The other fitting parameters are all constant and they are all shown in Table 4. The correlation coefficient R^2 of the regression formula is 99.88% for benzene on AC-0 and 99.86% for formaldehyde on AC-1, respectively. It can be seen that the breakthrough curve is very consistent with the Logistic model in formula (1), so the Logistic model fitting function can be used to predict the breakthrough curve.
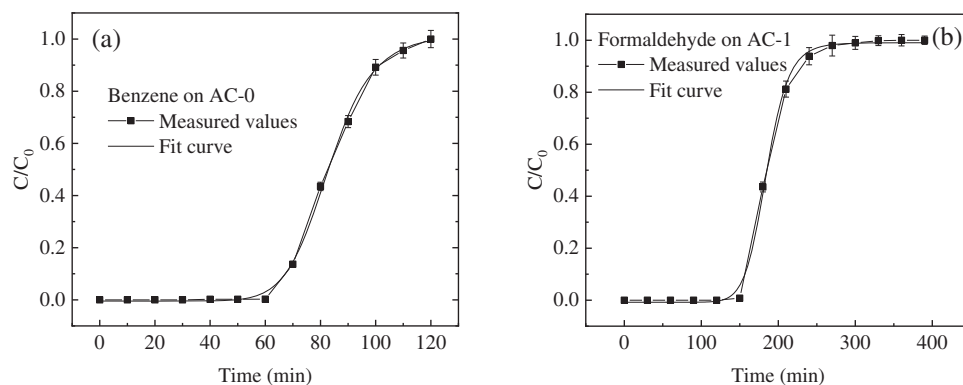

Figure 6: Normalized breakthrough curves of benzene on AC-0 activated carbon bed and formaldehyde on AC-1 activated carbon bed

Table 4: Parameters of the logistic model fitting function

Experiments	A_1	A_2	p	t_0
Benzene on AC-0	−0.004535	1.01535	10.2915	83.0176
Formaldehyde on AC-1	−0.00791	0.99048	12.81899	184.62305

Considering the influence of instrument and external conditions, 5% of inlet gas concentration is chosen as the breakthrough point, therefore the breakthrough time t_B can be calculated to be 63 min. When $t < 63$ min, the adsorption capacity of activated carbon at this stage is directly proportional to the adsorption time, which is the stage of activated carbon not saturated; from 63 to 125 min, the adsorption capacity of activated carbon is no longer proportional to the adsorption time. Both desorption and adsorption occur simultaneously during this period; $t > 125$ min, the adsorption, and desorption reached equilibrium. The concentration of benzene in the outlet gas was consistent with that in the inlet gas and the activated carbon bed was saturated. The saturated adsorption capacity of AC-0 for benzene at 30°C is 437.0 mg/g.

If the concentration of formaldehyde in the exhaust gas is 5% of that in the intake air, it is regarded as the breakthrough point, the breakthrough time t_C can be calculated to be 149 min by formula (1). When $t < 149$ min, the adsorption capacity of modified activated carbon at this stage is directly proportional to the adsorption time, which is the unsaturated stage of modified activated carbon, and the adsorption capacity at this stage is only related to the gas flow rate. In 149–300 min stage, the adsorption capacity of modified activated carbon is no longer proportional to the adsorption time. With the extension of time, desorption becomes more obvious, and the formaldehyde content in the outlet gas gradually increases;

when $t > 300$ min, the adsorption and desorption reached equilibrium, and the modified activated carbon bed was saturated finally. At this stage, the concentration of formaldehyde in the outlet air was consistent with that in the inlet air. The saturated adsorption capacity of AC-1 for formaldehyde at 30°C is 670.5 mg/g.

3.2.3 Saturated Adsorption Capacity of Samples at Different Temperatures

The relationship curves between Q/Q_0 and temperature are shown in Fig. 6. For benzene on AC-0, it can be seen from Fig. 6 that under normal atmospheric conditions, the rise/drop curves of the isobaric adsorption cycle basically coincide. It indicates that the system is always in the equilibrium state with equal adsorption and desorption rates under different temperature conditions. This phenomenon is the characteristic of physical adsorption, that is, the adsorption of benzene by activated carbon is a physical change, and the adsorption force is the van der Waals force [34,35]. When the temperature $T > 40$°C, the adsorption curve is approximate to a straight line, and the linear fitting equation is (the linear correlation coefficient is 99.3%),

$$\frac{Q}{Q_0} = -0.00461 \times (T + 273) + 1.996 \tag{2}$$

Thus, if the adsorption temperature increases to 150°C, the adsorption capacity of benzene will be 5% of that at 10°C (the saturated adsorption capacity at 10°C is 660 mg/g) based on the linear fitting equation. It indicates that the desorption regeneration operation may be carried out at 150°C by changing temperature, which has practical significance for industrial applications. Its regeneration rate is merely 71.2% if the adsorption temperature is 100°C. When the temperature $T < 40$°C, the adsorption curve is different from that at high temperatures, which is no longer a simple linear relationship, but the adsorption capacity increases rapidly with the decrease of temperature. It shows that the adsorption of benzene on activated carbon at low temperature is no longer the adsorption of the monolayer, but the phenomenon of multi-layer adsorption and condensation. Therefore, in order to obtain a better adsorption effect of activated carbon on benzene, the temperature should be lower than 40°C.

For formaldehyde on AC-1, it can be seen from Fig. 7 that the adsorption hysteresis phenomenon appears in the curve from 30°C to 90°C, which is obviously different from the adsorption of benzene. When comparing their adsorption curves, we can find that theformaldehyde in the pore cannot completely desorb under the same condition. In other words, rates of adsorption and desorption are not equal, which indicates a stronger adsorption affinity of this adsorbate to carbon surface in spite of its lower boiling point than that of benzenes. It shows that this adsorption is the result of chemical change [36–38]. The oxygen atom in formaldehyde molecules and the active groups in activated carbon form as hydrogen bonds, as shown in Fig. 5, and this is considered to bethe fundamental cause of the hysteresis. It is different from the independent domain theory or the network theory [39]. In order to desorb the adsorbed molecules, a higher temperature is needed; that is, adsorption is an exothermic process, conversely, desorption is an endothermic process. At 90°C, the formaldehyde adsorption capacity decreases to zero whereas benzene decreases down to about 145 mg/g and is caused by different boiling points. So, the desorption re generation operation can be carried out by changing the temperature to 90°C, whereas a higher temperature is necessary for benzene desorption.
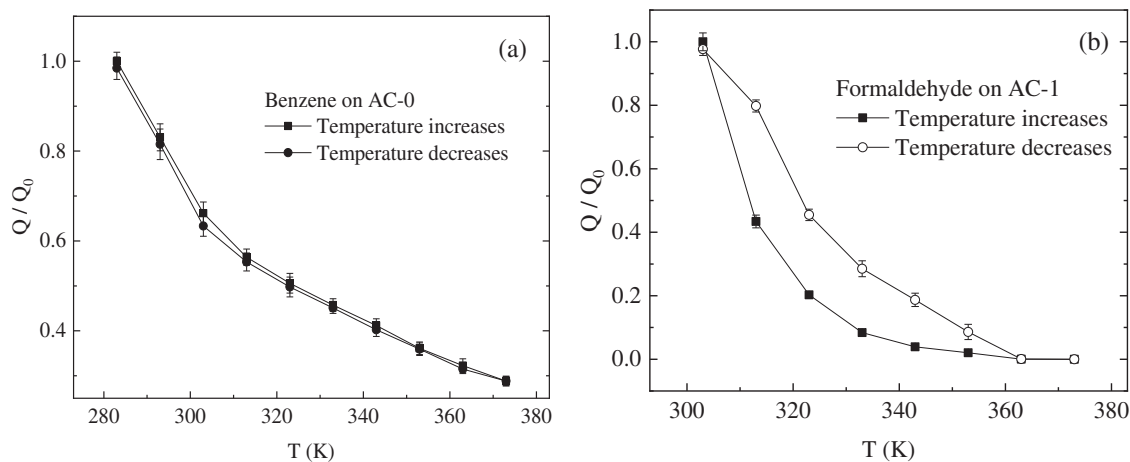
Figure 7: Normalized adsorption isobaric curves for benzene on AC-0 and formaldehyde on AC-1 under a normal atmosphere
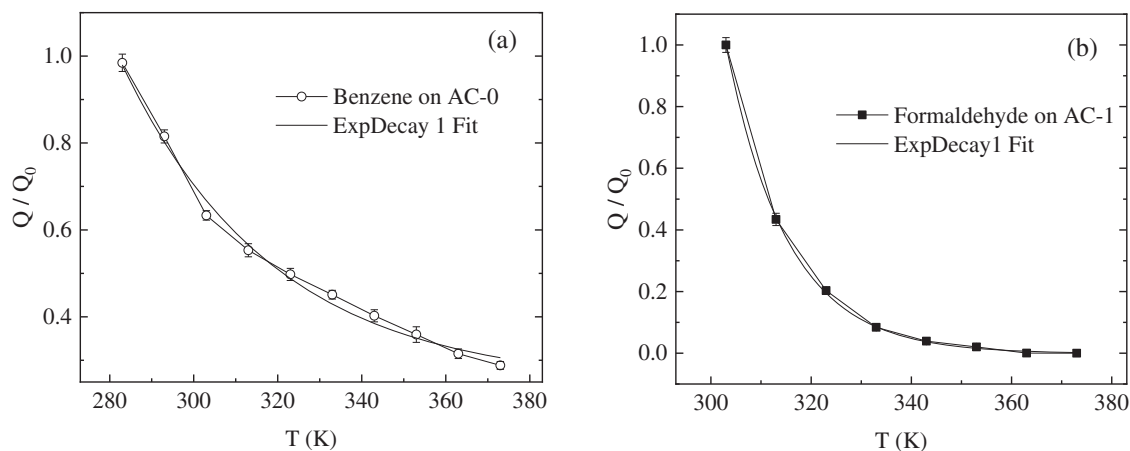

Figure 8: Adsorption isobaric curves from lower temperature to a higher one and their fitting curves

The adsorption isobaric curves from lower temperature to higher one are fitted by ExpDecay1 (the curves shown in Fig. 8) and the regression formula is as follows:

$$\frac{Q}{Q_0} = A e^{\frac{T_0 - T}{T_1}} + b \tag{3}$$

where Q/Q_0 is the normalized adsorption quantity when the temperature is T, Q_0 is the highest adsorption quantity under the experimental temperature, T is temperature, and other fitting parameters are all constant (they show in Table 5). The correlation coefficient R^2 of the regression formula is 99.06 for benzene on AC-0 and 99.96 for formaldehyde on AC-1. It is obvious that the two curves agree with ExpDecay1 very well for all test temperatures. Therefore, the fitted ExpDecay1 function can be used to calculate the adsorption isobaric process.

Table 5: The parameters of the fitting normalized adsorption isobaric curve equations

Experiments	b	A	$T_0(K)$	$T_1(K)$
Benzene on AC-0	0.24473	0.74319	282.59755	12.27724
Formaldehyde on AC-1	−0.00136	1.00275	302.96259	36.1929

4 Conclusion

Self-developed coconut shell activated carbon has a specific surface area of 1860 m^2/g and a pore size of 48.2 nm. The oxidation modification of potassium permanganate can reduce their values a little, but it can increase the oxygen-containing groups. Oxygen groups on the surface of activated carbon can improve the adsorption selectivity of compounds, which is good for polar molecules such as formaldehyde, but is not good for non-polar molecules such as benzene. The adsorption breakthrough curve in the activated carbon bed is very consistent with the Logistic model fitting function. At 30°C, the saturated adsorption capacity of AC-0 for benzene is 437.0 mg/g, and that of AC-1 for formaldehyde is 670.5 mg/g. The rise/fall temperature curves of benzene on the AC-0 adsorption bed basically coincide, and the linear correlation coefficient is 99.9%, indicating that the adsorption of benzene by coconut shell-activated carbon is physical adsorption. There is a desorption hysteresis in the rise/fall temperature curves of formaldehyde on AC-1, indicating that the adsorption of formaldehyde on AC-1 is chemical adsorption that forms hydrogen bonds. The regeneration operation of formaldehyde can be carried out at 90 °C under normal pressure, whereas the desorption of benzene requires a higher temperature.

Conflicts of Interest: The authors declare that they have no conflicts of interest to report regarding the present study.

References

1. Liu, S., Wang, B., He, J., Tang, X., Luo, W. et al. (2012). Source fingerprints of volatile organic compounds emitted from a municipal solid waste incineration power plant in Guangzhou, China. *Procedia Environmental Sciences, 12,* 106–115. DOI 10.1016/j.proenv.2012.01.254.

2. Zhang, X., Wang, D., Liu, Y., Cui, Y., Xue, Z. et al. (2020). Characteristics and ozone formation potential of volatile organic compounds in emissions from a typical Chinese coking plant. *Journal of Environmental Sciences, 95(9),* 183–189. DOI 10.1016/j.jes.2020.03.018.

3. Mursics, J., Urbancl, D., Goricanec, D. (2020). Process of formaldehyde and volatile organic compounds' removal from waste gases. *Applied Sciences, 10(14),* 4702. DOI 10.3390/app10144702.

4. Liang, Z., Wang, J., Zhang, Y., Han, C., Ma, S. et al. (2020). Removal of volatile organic compounds (VOCs) emitted from a textile dyeing wastewater treatment plant and the attenuation of respiratory health risks using a pilot-scale biofilter. *Journal of Cleaner Production, 253,* 120019. DOI 10.1016/j.jclepro.2020.120019.

5. Sinan, K. (2021). Excellent adsorptive performance of novel magnetic nano-adsorbent functionalized with 8-hydroxyquinoline-5-sulfonic acid for the removal of volatile organic compounds (BTX) vapors. *Fuel, 287(3–4),* 119691. DOI 10.1016/j.fuel.2020.119691.

6. Wang, F., Lei, X., Hao, X. (2020). Key factors in the volatile organic compounds treatment by regenerative thermal oxidizer. *Journal of the Air & Waste Management Association, 70(5),* 557–567. DOI 10.1080/10962247.2020.1752331.

7. Derylo-Marczewska, A., Blachnio, M., Marczewski, A., Swiatkowski, A., Buczek, B. (2017). Adsorption of chlorophenoxy pesticides on activated carbon with gradually removed external particle layers. *Chemical Engineering Journal, 308(1–3),* 408–418. DOI 10.1016/j.cej.2016.09.082.

8. Sultana, A. I., Saha, N., Reza, M. T. (2021). Synopsis of factors affecting hydrogen storage in biomass-derived activated carbons. *Sustainability, 13(4),* 1947. DOI 10.3390/su13041947.

9. Zorana, A., Gordan, S., Dragan, R., Boško, G., Nenad, R. et al. (2008). Low concentration volatile organic pollutants removal in combined adsorber-desorber-catalytic reactor system. *Hemijska Industrija, 62(2),* 51–58. DOI 10.2298/HEMIND0802051A.

10. Anil, K., Abhijeet, A., Priyanka, K. (2020). Production, activation, and applications of biochar in recent times. *Biochar, 2(3),* 253–285. DOI 10.1007/s42773-020-00047-1.

11. Shiue, A., Hu, S. C., Chang, S. M., Ko, T. Y., Hsieh, A. et al. (2017). Adsorption kinetics and breakthrough of carbon dioxide for the chemical modified activated carbon filter used in the building. *Sustainability, 9(9),* 1533. DOI 10.3390/su9091533.

12. Maurer, D. L., Koziel, J. A., Kalus, K., Andersen, D. S., Opalinski, S. (2017). Shiue (VOCs), and greenhouse gas emissions. *Sustainability, 9(6),* 929. DOI 10.3390/su9060929.

13. Wu, P., Ata-Ul-Karim, S., Pal, S. B., Wang, H., Wu, T. et al. (2019). A scientometric review of biochar research in the past 20 years (1998–2018). *Biochar, 1(1),* 23–43. DOI 10.1007/s42773-019-00002-9.

14. Shaarani, F., Hameed, B. (2010). Batch adsorption of 2,4-dichlorophenol onto activated carbon derived from agricultural waste. *Desalination, 255(1–3),* 159–164. DOI 10.1016/j.desal.2009.12.029.

15. Teixeira, S., Delerue-Matos, C., Santos, L. (2019). Application of experimental design methodology to optimize antibiotics removal by walnut shell based activated carbon. *Science of the Total Environment, 646,* 168–176. DOI 10.1016/j.scitotenv.2018.07.204.

16. Suo, F., Liu, X., Li, C., Yuan, M., Zhang, B. et al. (2019). Mesoporous activated carbon from starch for superior rapid pesticides removal. *International Journal of Biological Macromolecules, 121(12),* 806–813. DOI 10.1016/j.ijbiomac.2018.10.132.

17. Nemr, A., El-Sikaily, A., Khaled, A. (2010). Modeling of adsorption isotherms of Methylene Blue onto rice husk activated carbon. *Egyptian Journal of Aquatic Research, 36(3),* 403–425.

18. Hameed, B., Tan, I., Ahmad, A. (2008). Adsorption isotherm, kinetic modeling and mechanism of 2,4,6-trichlorophenol on coconut husk-based activated carbon. *Chemical Engineering Journal, 144(2),* 235–244. DOI 10.1016/j.cej.2008.01.028.

19. Belyaeva, O., Krasnova, T., Gladkova, O. (2015). Effect of the thermal treatment conditions of granulated active carbons on their properties. *Solid Fuel Chemistry, 49(3),* 196–200. DOI 10.3103/S0361521915030040.

20. Han, X., Lin, H., Zheng, Y. (2015). The role of oxygen functional groups in the adsorption of heteroaromatic nitrogen compounds. *Journal of Hazardous Materials, 297,* 217–223. DOI 10.1016/j.jhazmat.2015.04.056.

21. Ghaedi, M., Shojaeipour, E., Ghaedi, A., Sahraei, R. (2015). Isotherm and kinetics study of malachite green adsorption onto copper nanowires loaded on activated carbon: Artificial neural network modeling and genetic algorithm optimization. *Spectrochimica Acta Part A: Molecular and Biomolecular Spectroscopy, 142,* 135–149. DOI 10.1016/j.saa.2015.01.086.

22. Liou, T., Wu, S. (2009). Characteristics of microporous/mesoporous carbons prepared from rice husk under base- and acid-treated conditions. *Journal of Hazardous Materials, 171(1–3),* 693–703. DOI 10.1016/j.jhazmat.2009.06.056.

23. Zhou, Q., Duan, Y., Hong, Y., Zhu, C., She, M. et al. (2015). Experimental and kinetic studies of gas-phase mercury adsorption by raw and bromine modified activated carbon. *Fuel Processing Technology, 134,* 325–332. DOI 10.1016/j.fuproc.2014.12.052.

24. Yang, Z., Liu, X., Liu, X., Wu, J., Zhu, X. et al. (2021). Preparation of β-cyclodextrin/graphene oxide and its adsorption properties for methylene blue. *Colloids and Surfaces B: Biointerfaces, 200(1),* 111605. DOI 10.1016/j.colsurfb.2021.111605.

25. Al-Ghouti, M., Da'ana, D. (2020). Guidelines for the use and interpretation of adsorption isotherm models: A review. *Journal of Hazardous Materials, 393,* 122383. DOI 10.1016/j.jhazmat.2020.122383.

26. Boulinguiez, B., Le, C. P., Wolbert, D. (2008). Revisiting the determination of Langmuir parameters-application to tetrahydrothiophene adsorption onto activated carbon. *Langmuir, 24(13),* 6420–6424. DOI 10.1021/la800725s.

27. Hauchhum, L., Mahanta, P. (2014). Carbon dioxide adsorption on zeolites and activated carbon by pressure swing adsorption in a fixed bed. *International Journal of Hydrogen Energy, 5(4),* 349–356. DOI 10.1007/s40095-014-0131-3.

28. Parlayıcı, Ş., Pehlivan, E. (2017). Removal of metals by Fe_3O_4 loaded activated carbon prepared from plum stone (*Prunus nigra*): Kinetics and modelling study. *Powder Technology, 317,* 23–30. DOI 10.1016/j.powtec.2017.04.021.

29. Kannan, V., Arjunan, T., Vijayan, S. (2020). Experimental investigation of temperature swing adsorption system for air dehumidification. *Heat and Mass Transfer, 56(7),* 2093–2105. DOI 10.1007/s00231-020-02841-w.

30. Adam, J., Dario, M., Anton, L., Henrik, T., Srdjan, S. et al. (2020). Effects of bed aging on temperature signals from fixed-bed adsorbers during industrial operation. *Results in Engineering, 8,* 100156. DOI 10.1016/j.rineng.2020.100156.

31. Han, Z., Wang, D., Jiang, P., Sui, H., He, L. et al. (2020). Enhanced removal and recovery of binary mixture of n-butyl acetate and p-xylene by temperature swing-Vacuum pressure swing hybrid adsorption process. *Process Safety and Environmental Protection, 135,* 273–281. DOI 10.1016/j.psep.2020.01.019.

32. Yan, G., Song, Z., Yang, Z., Liu, X., Bai, Z. (2021). Study on adsorption of Benzene Gas on activated carbon prepared by low-temperature carbonization. *Applied Chemical Industry, 50(9),* 2432–2434+2439. DOI 10.16581/j.cnki.issn1671-3206.20210630.011.

33. Huang, J., Xi, B., Xv, Q., Wang, X., Li, W. et al. (2016). Experiment study of the effects of hydrodynamic disturbance on the interaction between the cyanobacterial growth and the nutrients. *Journal of Hydrodynamics, 28(3),* 411–422.

34. Zhang, X., Guo, J. (2022). Adsorption, stability and evolution path of benzene on graphene surface: Size and edge effects. *Applied Surface Science, 571,* 151376. DOI 10.1016/j.apsusc.2021.151376.

35. Qiao, Y., Lv, N., Li, D., Li, H., Xue, X. et al. (2021). Construction of MOF-shell porous materials and performance studies in the selective adsorption and separation of benzene pollutants. *Dalton Transactions, 50(26),* 9076–9087. DOI 10.1039/D1DT01205C.

36. Tran, T. Y., Younis, S. A., Heynderickx, P. M., Kim, K. (2022). Validation of two contrasting capturing mechanisms for gaseous formaldehyde between two different types of strong metal-organic framework adsorbents. *Journal of Hazardous Materials, 424(1),* 127459. DOI 10.1016/j.jhazmat.2021.127459.

37. Zhu, J., Chen, J., Zhuang, P., Zhang, Y., Wang, Y. et al. (2020). Efficient adsorption of trace formaldehyde by polyaniline/TiO_2 composite at room temperature and mechanism investigation. *Atmospheric Pollution Research, 12(2),* 1–11. DOI 10.1016/j.apr.2020.09.015.

38. Liu, L., Liu, J., Zeng, Y., Tan, S. J., Do, D. D. et al. (2019). Formaldehyde adsorption in carbon nanopores – New insights from molecular simulation. *Chemical Engineering Journal, 370,* 866–874. DOI 10.1016/j.cej.2019.03.262.

39. Mason, G. (1983). A model of adsorption-desorption hysteresis in which hysteresis is primarily developed by the interconnections in a network of pores. *Proceedings of the Royal Society A: Mathematical Physical and Engineering Sciences, 390(1798),* 47–72. DOI 10.1098/rspa.1983.0122.